



RELIABILITY APPROACH FOR THE BEHAVIOUR OF ADHESIVELY-BONDED ASSEMBLIES IN MARINE APPLICATIONS

Mejri M.*, Cognard J.-Y. *, Davies P.**

* Mechanics of Naval and Offshore Structures, ENSIETA, 29806 Brest Cedex 09, France

** Materials and Structures group, IFREMER Centre of Brest, 29280 Plouzané, France

Keywords: Adhesively-bonded assemblies, Composites, TDCB specimens, Cohesive-zone models, Damage, Time-variant reliability.

Abstract

In order to reduce the time and cost of mechanical design nonlinearities must be included when simulating the behaviour of a structure; this leads to nonlinear finite element simulations in the case of industrial structures. Moreover we have to take into account the random and temporal character of loads and other parameters.

The objective of this paper is to propose a time variant reliability approach for adhesively bonded assemblies in marine application. The proposed strategy requires the combination of time variant reliability and non linear finite element analysis. This study takes into account the random and temporal character of material behaviour, environmental conditions and loads. To demonstrate the feasibility and the difficulties of such a combination, an example focusing on adhesively-bonded assemblies is proposed. In order to limit numerical costs, cohesive zone elements are used to model the non linear behaviour of the adhesive joint. Results from the PHI2 method and comparison between two variants of this time variant reliability method are presented.

1 Introduction

Assembling elements of composite structures or metallic materials by adhesively bonding allows improved productivity by simplifying design constraints. It can also lead to significant weight gain. However, some design offices lack confidence in this approach, which limits the use of this technology today. For naval applications the manufacturing conditions are characterized by relatively thick adhesive joints (at least 0.5 mm),

joining of large-sized parts, simple preparation of surfaces and post cure at a low temperature. Moreover, some parameters are not completely controlled, such as: geometry of the edges of the adhesive joint, joint thickness variations, adhesive lack in some zones...

The assessment of risks stemming from these phenomena is an essential issue in predicting the service life. The adhesive behaviour can in general be represented by viscoplastic models with irreversible damage; its mechanical characteristics evolve with time and naval structures are subjected to stochastic loadings. Under these assumptions, time-independent reliability does not provide sufficiently relevant and realistic information, it is thus necessary to use the theory of time-dependent reliability to take into account the time dependence of the phenomena and the loadings.

Coupling the structural reliability software evaluation with a non-linear finite element analysis requires robust mechanical models to ensure the durability of a structure in time.

The use of cohesive-zone models and interface elements allows the mesh dependence to be limited for the study of the crack propagation in the adhesive. The first goal is to evaluate the impact of the random parameters on the lifetime of adhesive bonded joints for naval applications. Moreover this approach, using cohesive models, takes into account the effect of adhesive degradation particularly close to defects. Initial defects in the adhesive joint can be modeled by introducing initial damage.

2 Reliability analyses

Reliability evaluation of an ageing structure needs to focus attention on the temporal and random character of material properties, environmental

conditions and loadings. To the extent that naval structures are concerned, some design parameters and their evolution in time are not completely mastered. In the case of assembling elements of composite structures or metallic materials by adhesive bonded joints, variability in joint thickness or adhesive cure can not be ignored. Thus, taking it into account from the design of this structure can result in improved service life.

A realistic prediction of the behaviour of a structure, particularly in maritime applications, requires considering non-linear structural response. This requires non-linear finite element analysis, which is nowadays widely recognized as the most effective method to assess the response of industrial-type structures. Its combination with time-variant reliability methods is thus a way to optimize their maintainability.

The classical approach for time-variant reliability analysis relies on the computation of out-crossing rates (of the limit-state surface). Among the existing methods, the PHI2 method ([1], [2]) is interesting as it allows the use of time-independent reliability methods such as FORM (First-Order Reliability Method). In this paper, the reliability analysis is performed by the software PHIMECA® [3] which enables the combination with the finite element software CAST3M® [4]. The feasibility of the combination between time-variant reliability and non-linear finite element analysis for solicitations representative of marine structures was shown in [5].

3 Time-variant reliability methods

The main points of the reliability methods are recalled in this section.

3.1 The PHI2 method

The set of random variables used in the mechanical problem is defined as $\mathbf{X}(t, \omega)$, t being the studied time and ω standing for the outcome in the space of outcomes Ω . Time-dependent limit-state function $\mathbf{G}(t, \mathbf{X}(t, \omega))$ is defined to perform the reliability analysis. This function divides the space of outcomes into two areas: the safe domain $\mathbf{G}(t, \mathbf{X}(t, \omega)) > 0$ and the failure domain $\mathbf{G}(t, \mathbf{X}(t, \omega)) \leq 0$. The frontier between these two domains is defined by $\mathbf{G}(t, \mathbf{X}(t, \omega)) = 0$ and called the limit-state surface. Performing a time-independent reliability analysis corresponds to the

assessment of the probability that the structure fails at time T :

$$P_{f,i}(T) = \text{prob}(\mathbf{G}(\tau, \mathbf{X}(\tau, \omega)) \leq 0) \quad (1)$$

We can also define the cumulative probability of failure $P_{f,c}$, which, under the hypothesis of a regular process, corresponds to the assessment of the probability that the structure fails within $[0, T]$. This probability of failure can be written as:

$$P_{f,c}(0, T) = \text{prob}(\exists \tau \in [0, T] \text{ such as } \mathbf{G}(\tau, \mathbf{X}(\tau, \omega)) \leq 0) \quad (2)$$

However, when the limit-state function \mathbf{G} decreases in the interval $[0, T]$, then, for each time $\tau \leq T$, cumulative and instantaneous probability of failure are equal:

$$P_{f,c}(0, \tau) = P_{f,i}(\tau) \quad (3)$$

To perform time-variant reliability analysis, we can also compute the out-crossing rate of the process under consideration through the limit-state surface. This out-crossing rate can be defined by:

$$v^+(t) = \lim_{\substack{\Delta\tau \rightarrow 0, \\ \Delta\tau > 0}} \frac{\text{Prob}(A \cap B)}{\Delta\tau} \quad (4)$$

$$\text{where} \begin{cases} A = \{\text{Structure in the safe domain at } t\} \\ = \{\mathbf{G}(t, \mathbf{X}(t, \omega)) > 0\} \\ B = \{\text{Structure in the failure domain at } t + \Delta\tau\} \\ = \{\mathbf{G}(t + \Delta\tau, \mathbf{X}(t + \Delta\tau, \omega)) \leq 0\} \end{cases}$$

The cumulative probability of failure can thus be bounded by ([6], [7]):

$$\max_{0 \leq t \leq T} [P_{f,i}(t)] \leq P_{f,c}(0, T) \leq P_{f,i}(0) + \int_0^T v^+(t) dt \quad (5)$$

The PHI2 method [1], used to compute the out-crossing rate, considers the estimation of the probability in Eq.(4) as a two-component parallel system analysis. The advantage of this method is that only needs time-independent reliability tools. Indeed, in this method, time is frozen and becomes a simple parameter (figure 1).

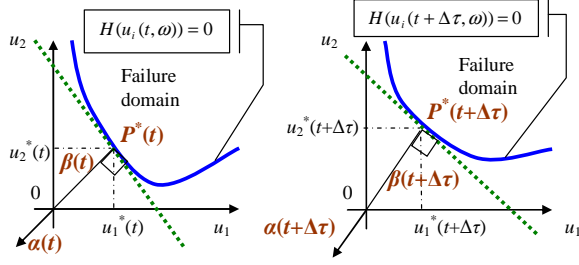


Fig. 1. Evolution of the reliability products during $\Delta\tau$.

If FORM is used for the reliability analysis, two successive analysis gives the coordinates of the tangent hyper-plane to the limit-state surface at time t and $t + \Delta\tau$. The correlation between the two events $A = \{\mathbf{G}(t, \mathbf{X}(t, \omega)) > 0\}$ and $B = \{\mathbf{G}(t + \Delta\tau, \mathbf{X}(t + \Delta\tau, \omega)) \leq 0\}$ is denoted by:

$$\rho_{\mathbf{G}\mathbf{G}}(t, t + \Delta\tau) = -\mathbf{a}(t) \cdot \mathbf{a}(t + \Delta\tau) \quad (6)$$

The first order evaluation of the probability of failure of the parallel system is then:

$$\text{Prob}(A \cap B) = \Phi_2(\beta(t), -\beta(t + \Delta\tau), \rho_{\mathbf{G}\mathbf{G}}(t, t + \Delta\tau)) \quad (7)$$

Φ_2 being the repartition function of the binormal law. The out-crossing rate follows:

$$v_{PHI2}^+(t) = \frac{\Phi_2(\beta(t), -\beta(t + \Delta\tau), \rho_{\mathbf{G}\mathbf{G}}(t, t + \Delta\tau))}{\Delta\tau} \quad (8)$$

In this expression, the choice of $\Delta\tau$ is fundamental; this choice is developed in [8]. To make possible this choice, Sudret [2] has recently improved the method by reconsidering formulation of Eq. (4). By introducing the following quantity:

$$f_t(\Delta\tau) = \text{Prob}(\{\mathbf{G}(t, \mathbf{X}(t, \omega)) > 0\} \cap \{\mathbf{G}(t + \Delta\tau, \mathbf{X}(t + \Delta\tau, \omega)) \leq 0\}) \quad (9)$$

Since $f_t(0) = 0$, Eq. (4) can be rewritten as:

$$v_{PHI2}^{+, \text{new}}(t) = \lim_{\Delta\tau \rightarrow 0} \frac{f_t(\Delta\tau) - f_t(0)}{\Delta\tau} = \left. \frac{df_t(\Delta\tau)}{d\Delta\tau} \right|_{\Delta\tau=0} \quad (10)$$

Introducing the notation:

$$\Psi(x) = \varphi(x) - x \cdot \Phi(-x) \quad (11)$$

The out-crossing rate can be developed as:

$$v_{PHI2}^{+, \text{new}}(t) = \|\tilde{\alpha}'(t)\| \cdot \varphi(\beta(t)) \cdot \Psi\left(\frac{\beta'(t)}{\|\tilde{\alpha}'(t)\|}\right) \quad (12)$$

Both expressions of the out-crossing rate are compared in the sequel.

3.2 Methodology of the combination

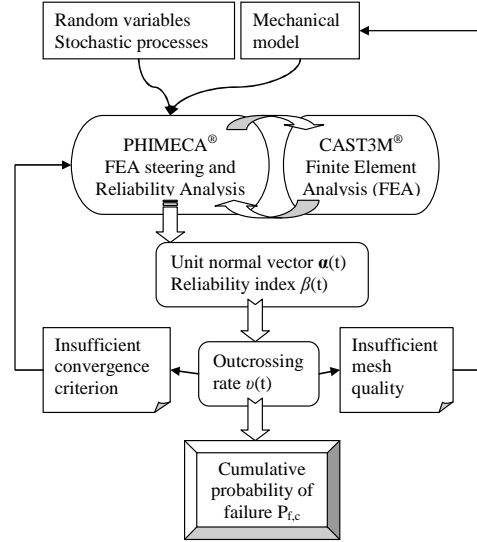


Fig. 2. Implementation scheme of the combination

Figure 2 shows the implementation scheme of the direct combination of time-variant reliability methods with finite element analysis. The mechanical model, random variables and stochastic processes are defined in PHIMECA®. To compute the mechanical model during the reliability analysis, PHIMECA® requires finite element computation (done with the finite element software CAST3M®). When convergence criteria of the reliability algorithm are reached, the unit normal vector $\alpha(t)$ and the reliability index $\beta(t)$ are obtained. Then PHI2 method is used to compute the out-crossing rate $v(t)$. This assessment can be inaccurate due to convergence criteria of the reliability algorithm or due to insufficient quality of the finite element mechanical model in the iterative procedure used for non-linear problems. In this case, the combination has to be run again until obtaining an out-crossing rate that allows an accurate assessment of the cumulative probability of failure $P_{f,c}$. Further work on parameters optimization has to be done in a second step. One of the crucial issues in a reliability study is the computational time cost which is directly proportional to the number of calls to the

limit-state function (each one representing a non-linear finite element analysis). For our study, the Abdo-Rackwitz algorithm together with the Newton-Raphson line-search method showed the best efficiency with respect to this consideration. To find the best compromise between numerical cost and precision of the results, the designer has to deal with convergence criteria, either in the reliability analysis or in the F.E. procedure. As far as this study is concerned, work was done mainly on:

- The ratio between the limit-state function at iteration $k+1$ and the initial limit-state function (assessed for the reliability algorithm starting point): $|G(x_{k+1})/G(x_0)|$;
- The difference between reliability indexes at two successive iterations k and $k+1$: $|\beta_{k+1} - \beta_k|$;
- Parameters of the line-search method during the reliability analysis;
- Precision on residual forces during the iterations of the non-linear F.E. incremental procedure (Newton type algorithm).

4 Mechanical model

If we consider a bonded structure composed of two elastic bodies joined by a plane adhesive layer; it is natural to model the adhesive with an interface element placed between solid bodies. This approach is based on a Dugdale-Barenblatt cohesive zone.

When the cohesive zone size is negligible compared with the assembly dimensions [9] we can model the interface with a zero thickness entity (figure 3) between the two substrates Ω_+ and Ω_- .

Introducing a damage model allows us to model delamination initiation and propagation at the interface. Using a zero thickness surface to represent the cohesive zone implies that the delamination propagation zone will be reduced. The used numerical model is written in a parametric way, which allows us to retrieve, for a specific set of parameters, the Tvergaard, Allix et al. or Alfano et al. [10] models.

The constitutive equation of the interface elements is established in terms of relative displacements (displacement discontinuities) and the interface tractions. In the following \mathbf{n} is the normal direction to the interface (adhesive joint).

$$\begin{aligned} [U] &= U^+ - U^- = [U_n] \bar{\mathbf{n}} + [U_s] \bar{\mathbf{s}} \\ \bar{\mathbf{t}} &= t_n \bar{\mathbf{n}} + t_s \bar{\mathbf{s}} \end{aligned} \quad (13)$$

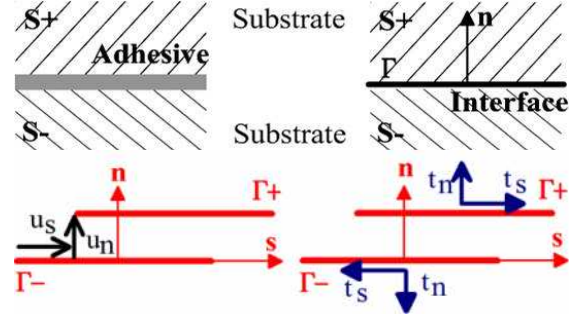


Fig.3. Interface modeling

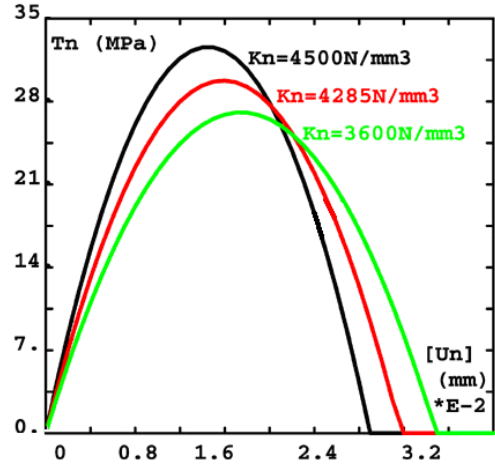


Fig.4. Traction model response

In the chosen model (Valoroso et al. [11]), the damage occurs when the joint is loaded in tension or shear, and it will be constant if the loading is compressive. The state laws are obtained from the following thermodynamic potential:

$$\Psi([u], D) = \frac{1}{2} (1-D) [K_n^+ \langle [U_n] \rangle_+^2 + K_s \langle [U_s] \rangle^2] + \frac{1}{2} K_n^- \langle [U_n] \rangle_-^2 \quad (14)$$

$$\begin{aligned} t &= \frac{\partial \Psi}{\partial [u]} = K_n^- \langle [U_n] \rangle_- \bar{\mathbf{n}} + \\ &(1-D) [K_n^+ \langle [U_n] \rangle_+ \bar{\mathbf{n}} + K_s \langle [U_s] \rangle \bar{\mathbf{s}}] \end{aligned} \quad (15)$$

$$\begin{aligned} Y_m &= -\frac{\partial \Psi}{\partial D} \\ &= \frac{1}{2} K_n^+ \langle [U_n] \rangle_+^2 + \frac{1}{2} K_s [U_s]^2 \\ &= \frac{1}{2} K_n^+ \left(\langle [U_n] \rangle_+^2 + \alpha^2 [U_s]^2 \right) \end{aligned} \quad (16)$$

We can also write the damage driving force as:

$$Y_m = \frac{1}{2} K_n^+ \delta^2$$

$$\text{with } \delta^2 = \left(\langle U_n \rangle_+^2 + \alpha^2 [U_s]^2 \right) \quad (17)$$

Where $\langle X \rangle_+ = 0.5 * (X + |X|)$ indicates the positive part of X. D, denotes the damage internal variable. K_n^+ and K_s are respectively the normal and tangential damaged stiffness and K_n^- is the compressive undamaged interface stiffness.

$\alpha = \sqrt{K_s / K_n^+}$: quantifies each mode contribution. Parameter γ denotes the mixity ratio. We can write the contribution of modes I and II as:

$$\gamma = \alpha \left[\frac{[U_s]}{\langle [U_n] \rangle_+} \right]; \quad Y_I = \frac{1}{1 + \gamma^2} Y_m$$

$$Y_{II} = \frac{\gamma^2}{1 + \gamma^2} Y_m \quad (18)$$

The damage evolution law and energy release rates in modes I and II are expressed, if we consider Y_m^* the critical thermodynamic damage driving force in mixed mode, as:

$$\phi_m = Y_m - Y_m^* \leq 0; \quad \dot{D} \geq 0; \quad \phi_m \dot{D} = 0$$

$$G_i = \int_0^\infty Y_i \dot{D} dt; \quad i \in \{I, II\} \quad (19)$$

G_i represents the critical energy release rate in mode $i \in \{I, II\}$. Figure 4 presents the traction response of this model. That choice has been made for the following model parameters: $K_n \in [3600, 4500] \text{ N/mm}^3$, $\alpha = 1.6$, $G_I = 630 \text{ J/m}^2$

5 Experimental approaches

5.1 TDCB specimen

Analyses of delamination growth apply a fracture mechanics approach and evaluate the energy releases rates in each mode; this energy, which describes the ability of a material containing a crack to resist fracture, is a property of the material. Different experimental devices exist to determine the energy release rate in mode I ([12-14]); the

TDCB (tapered double cantilever beam) protocol will be retained here to characterize the adhesive on metallic substrates. One of the characteristics of this protocol is that we obtain a crack propagation at a constant applied load. Three methods were explored to analyze the TDCB experimental results: the SBT (simple beam method), the CBT (corrected beam theory) and the ECM (experimental compliance method) [15]. For numerical simulation we will retain the mean value obtained by these three methods. Figure 6 shows the critical energy release rate obtained for aluminum alloy substrate bonded with araldite 2015, the total specimen length is about 310 mm and an initial crack of 50 mm is introduced. The adhesive bond-line thickness is 1 mm.



Fig.5. Experimental TDCB specimen

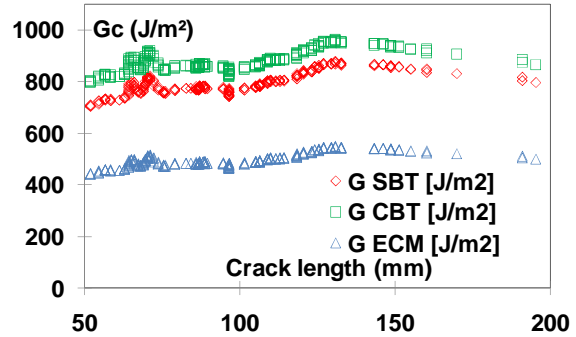


Fig.6. Critical energy release rate

Experimental tests have also been performed with steel substrates, and similar results were found.

5.2 Composite specimens

In order to characterize adhesively bonded composite substrates with the same adhesive, the parallel sided DCB specimen was employed. Figure 7 shows the specimen and figure 8 shows results for a 1mm joint thicknesses. These are thick bond lines but are representative of the thicknesses found in naval construction where large composite parts with possible dimensional variations are assembled. The

substrates are infusion moulded 0/90° glass reinforced vinyl ester composites. Mode I delamination energies around 600 J/m² are again obtained during propagation, using a compliance calibration data reduction scheme.

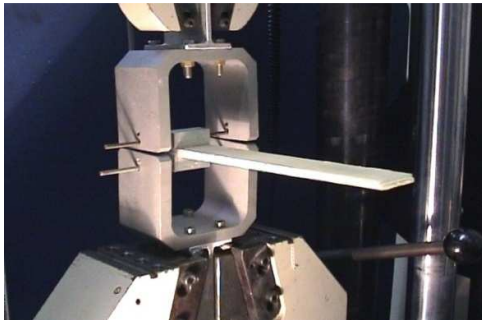


Fig.7. Composite DCB specimen

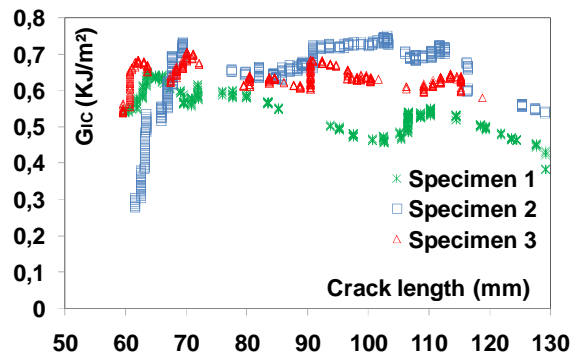


Fig.8. Critical energy release rate, 3 bonded DCB specimens

5.3 Numerical analyses

The TDCB was modeled with the CAST3M® Finite Element Code, using the cohesive model presented in the previous paragraph.

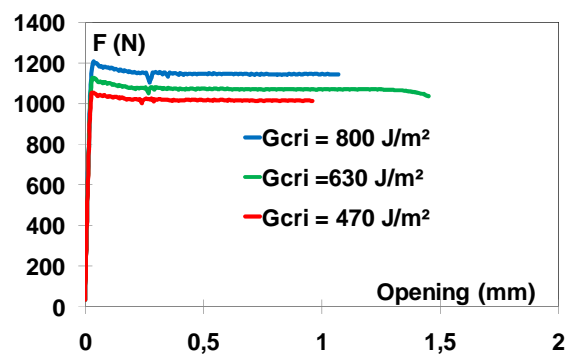


Fig.9. R curve sensibility to critical energy release rate

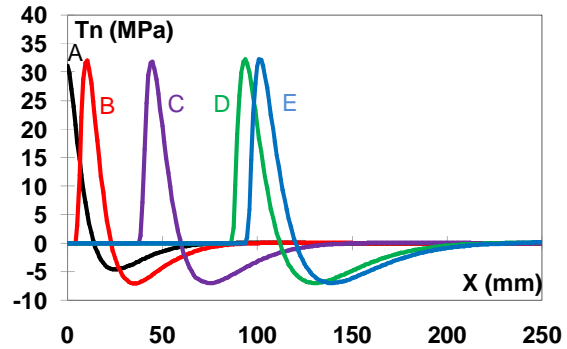


Fig.10. Normal stress evolution versus crack length.

As a first step, we performed a parametric study for different values of energy release rate. Figure 9 represents the loading force versus crack opening ($G_I \in [630, 800]$ J/m²). We note that numerical and experimental results are in good agreement (experimental measured load was about 900 N). Figure 10 shows normal stress evolution versus crack propagation for $G_I = 470$ J/m² (A, B, C, and D represent different times during the test). It may be noted that the crack advance occurs for a constant value of normal stress. The numerical computation was done with a mesh with 300 joint elements. It may also be noted that the stress value is zero for already cracked elements, maximal for the crack front and becomes a compressive stress for the elements in front of the crack.

6 Reliability analyses

6.1 Presentation of the numerical example

In order to study a representative joining problem of marine application, our example should have a low numerical cost, be able to take into account the crack propagation and model the degradation of the adhesive joint. The chosen model should also be able to give a correct description for the state of the structure during the load path. As a consequence, the adhesive layer is modeled with cohesive zone elements. In order to avoid interpenetration between the two parts of the cracked structure, contact conditions are added because they are not included directly in the material model. The example (figure 11) consists of two rectangular aluminum plates (Young modulus: $E = 67000$ Mpa, $\nu = 0.34$, $a = 100$ mm, $b = 5$ mm) connected by an adhesive joint, the joint is modeled with 400 cohesive elements. The material model for the adhesive has been presented before. The load is

prescribed on the border: Dy is vertical displacement.

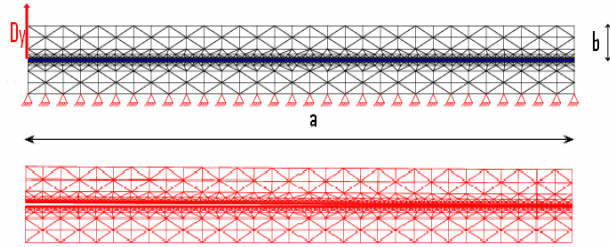


Fig. 11. Studied example

As example figure 12 presents the evolution of the state of damage of the adhesive joint for different values of the prescribed displacement Dy . The figure shows the evolution of crack propagation (associated with $D = 1$) with respect to the prescribed loading.

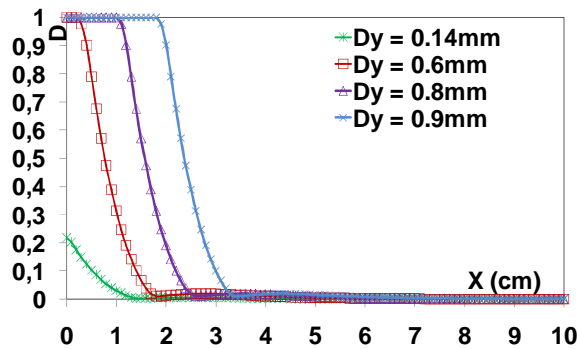


Fig.12. Damage evolution in time (deterministic case)

Computations are made on a Pentium IV 3 GHz with 1 Gb RAM. Preliminary works shows the necessity to make a compromise between mesh qualities, time step, number of variable and quality of numerical results. Four random parameters are retained to perform the study; the first one is the length of the beam which is a geometric variable, normal stiffness and critical energy release rate represents some aspect of random on the adhesive; the fourth variable which is the vertical prescribed displacement represents the load variable.

Table 1. Random variables distributions

Variable	Distribution	Mean	St-dev
a (mm)	Normal	100	10%
Kn (N/mm ³)	Normal	6350	10%
G (J/mm ²)	Normal	0.470	10%
Dy (mm)	Normal	0.8	10%

Two limit state functions will be studied at the sequel, the first one is based on the computation of the average of damage of the bonding joint and the second one is in relation with the evolution of the stiffness of the assembly which takes into account the crack closure.

6.2 Limit state function based on damage average

The first choice of the failure criterion which is associated, at a given instant, to the average of the damage values on the cohesive zone; the function of performance can be written as following:

$$G(t) = D_{Threshold} - D_{mean} \quad (20)$$

with

$$D_{mean} = \int_{\text{bonding joint}} D(x) dx / \int_{\text{bonding joint}} dx$$

$$D_{Threshold} = 0.24 \quad (21)$$

$D_{Threshold}$ characterizes the maximum mean damage value admissible for the joint of adhesive. The value of 0.24 is chosen as example and characterizes a lost of the rigidity of the bonded assembly for about 30%. Its numerical value does not affect the algorithm behaviour.

A comparative between two prescribed vertical displacements is made. The first displacement evolves linearly in time and the second one has no constant speed evolution. Prescribed displacements are presented on figure 13. The objective is to evaluate the influence of time description of the prescribed loads (in particular, the influence of a slow variation in time of the loading). A time step of 3s is used in computation and interval of study is limited to [300s, 360s] (i.e. 120 increments or the non linear F.E simulation).

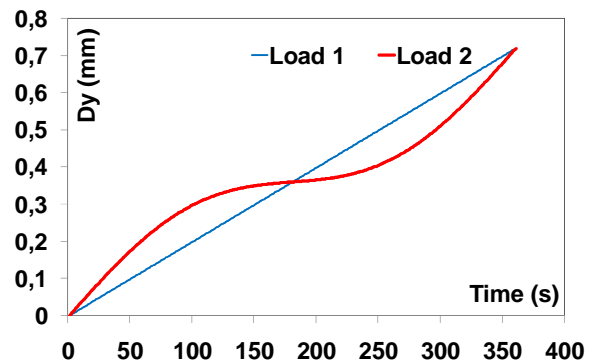


Fig.13. Time evolution of prescribed displacements

The average of the damage is increasing in time, this condition ensures the decreasing of function of limit state $G(t)$, this condition ensures the equality between $P_{f,i}$ and $P_{f,c}$ and a comparative study can be made, we can also define the relative errors $err_{P_f}(t)$ to evaluate the assessment accuracy as:

$$err_{P_f}(t) = \frac{P_{f,c}(t) - P_{f,i}(t)}{mean(P_{f,c}(t); P_{f,i}(t))} \quad (22)$$

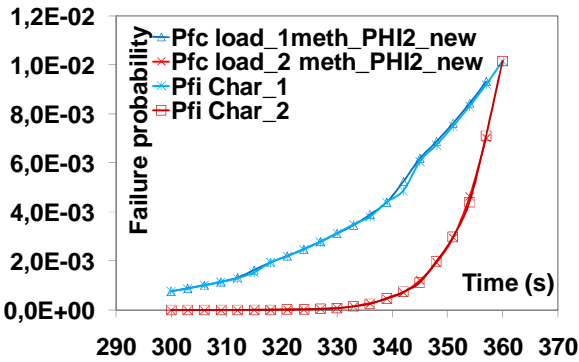


Fig. 14. Cumulative and instantaneous probabilities of failure (loading time step 3s)

Failure probability obtained for the two loading configurations are presented on figure 14, it's important to note that we obtain a good accuracy between $P_{f,c}$ and $P_{f,i}$, and a same final failure probability is obtained for the two displacements configurations.

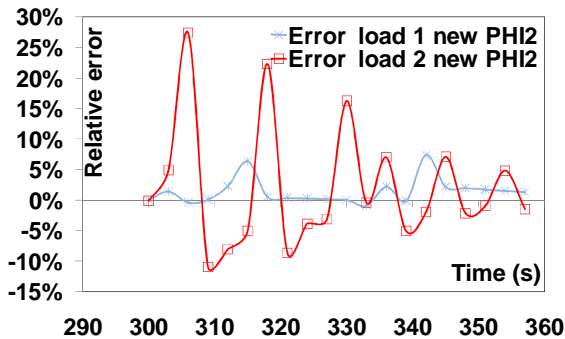


Fig.15. Error estimation on the assessment of $P_{f,c}$ for the two loadings

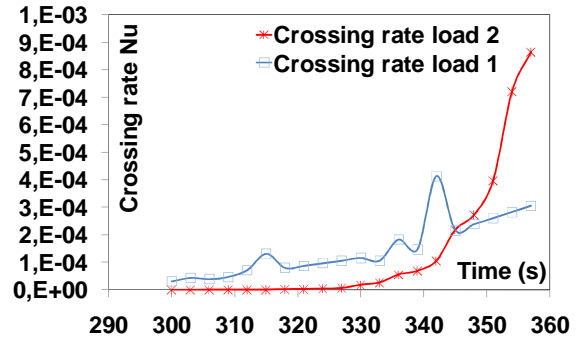


Fig.16. Crossing rate evolution

If we focus attention on the error estimation we observe that the second load configuration presents some little fluctuations, this phenomena is due to the low increase of loading which can increase some error at each time step of the non linear F.E calculation (figure 15). Time step was divided by three in order to reduce this problem (figure 17), results are presented for the interval [300s, 340s]

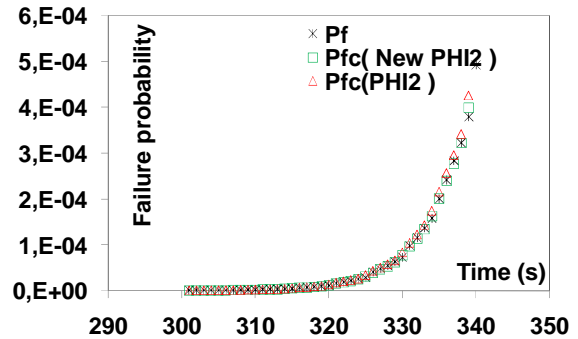


Fig.17. Reliability analysis: comparative between $P_{f,c}$ loading time step 1s, load configuration 2

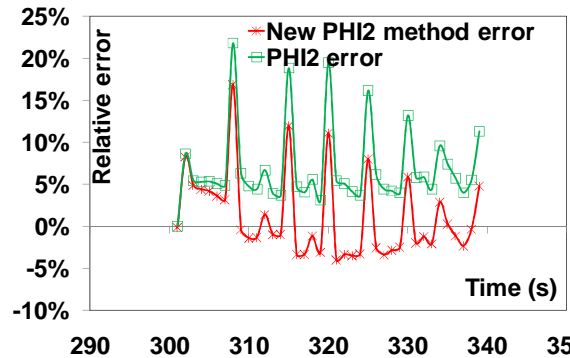


Fig.18. Reliability analysis: comparative between relative errors

It seems that if the precision of finite element computation remain the same, the fluctuations are still there. In order to increase the precision of the results we have to increase numerical finite elements and reliability computation precision. It's also important to note that the use of the second variant of the PHI2 method to compute the cumulative probability of failure $P_{f,c}$ gives better results. The old PHI2 method clearly over-evaluates the cumulative probability of failure.

It's important to note that computation times are about four hours for each $P_{f,i}$ computation. It's clear that such problem has a quite low numerical cost. It is important to note that the objective of this study is to analyze the precision of such reliability analysis.

6.3 Limit state function based on the estimation of the stiffness of bonded structure

The first limit state function which is based on the damage computation is one way to take into account the evolution of the stiffness of a bonded structure in time, however if we solve a problem with crack closure, this criterion don't takes into account this phenomena; in fact damage is always increasing (or constant), however if crack is closed the stiffness of the assembly is modified. A second limit state function taking into account the difference between closure and opening of cracks is proposed. This limit state function based on stiffness evolution can be written such as:

$$G(t) = R_{Threshold} - R_{eq} \quad (23)$$

$$R_{eq} = \int_{\text{bonding joint}} \delta(x)D(x)dx / \int_{\text{bonding joint}} dx$$

$$R_{Threshold} = 0.2 \quad (24)$$

Where $\delta(x)$ is defined such as:

$$\text{If } [U_n] > 0: \delta(x) = 1 \text{ else } \delta(x) = 0 \quad (25)$$

In other words, damage will be considered only if the crack is open, other wise, if we are working on crack closure damage will not be considered. The propound example shows the interest of such criterion especially for a case of loading which gives a limit state function which is not decreasing in times. The same structure with the same set of random parameters is considered. The prescribed vertical displacement and the associated limit state evolution are presented in the following figure.

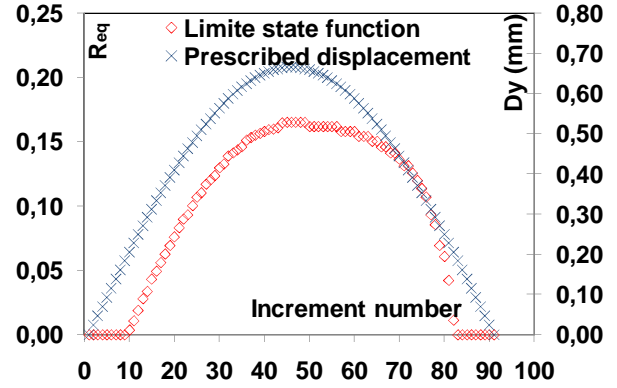


Fig.19. Second limit state representative

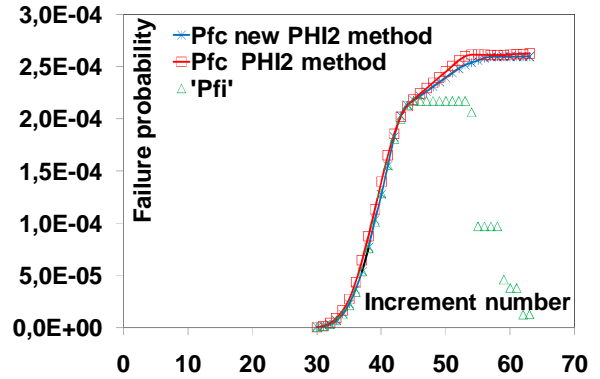


Fig.20. PHI2 method: comparison between relative errors

Cumulative probability of failure and instantaneous one differs. In this case, evaluating $P_{f,i}$ is not sufficient; PHI2 method is used to evaluate the failure probability. We have to note that the crossing rate is constant when the reliability index $\beta(t) = \beta(t+dt)$, then it is equal to zero for $\beta(t) < \beta(t+dt)$. Numerical tests are underway to complete this study. Moreover variants of the propounded state function can be proposed in order to take into account the effects of modes I and II.

7 Conclusions

This paper presents an example of combination between time-variant reliability methods and non-linear finite element analysis; time-variant reliability analysis was realized by the PHI2 method and the two existing formulations are compared. It presents also a comparative between two state limit functions; the influence of a slow variation in time of the loading on the $P_{f,c}$ results has been studied. The second example, associated with a limit state

function based on the estimation of the stiffness of the assembly shows the interest of the time variant reliability when solving problems dealing with crack opening and crack closure.

The proposed approach allows modeling the degradation of a bonded joint by taking into account the initial defects. The compatibility of this approach with stochastic phenomena makes it attractive to solve engineering problems. Some aspect like the difficulties to obtain good accuracy in the results, especially when stochastic processes are involved, shows that we have to find compromise between calculation cost and results precision. Further works are underway, in order to reduce the numerical cost of such simulation involving strong non linearities linked with damage evolution and cracks for industrial application of bonding (T-Bonded structure).

Acknowledgements

These studies are funded by the Bretagne Region.

References

- [1] Andrieu-Renaud, C., Sudret, B. & Lemaire, M. "The PHI2 method: A way to compute time-variant reliability". *Reliability Engineering and System Safety* Vol. 84: pp. 75-86, 2002.
- [2] Sudret, B. "Analytical derivation of the outcrossing rate in time-variant reliability problems". *Reliability and Optimization of Structural Systems*. 12th WG 7.5 IFIP Conference, Aalborg, Denmark, 2005.
- [3] PHIMECA® Engineering S.A. "Manuel d'utilisation PHIMECA Software Version 1.6", 2003.
- [4] CAST3M® "Cast3m: Documentation". EUROSIM / CEA SEMT, 2004..
- [5] Cazuguel, M., Renaud, C. & Cognard, J.Y. "Time-variant reliability of non-linear structures: Application to a representative part of a plate floor". *Quality and Reliability Engineering*, Vol. 22 (special issue on Maritime Risk Modeling and Decision Making): pp. 101-118, 2006.
- [6] Li, C.C. & Der Kiureghan, A. 1993. 'Optimal discretization of random fields'. *Journal of Engineering Mechanics* Vol. 119 (No. 6): pp. 1136-1154.
- [7] Sudret, B. & Der Kiureghan, A. 'Stochastic Finite Element Methods and Reliability. A State-of-the-Art Report'. Report No. UCB/SEMM-2000/08, University of California, Berkeley, 2000.
- [8] Andrieu, C., Lemaire, M. & Sudret, B. 2002. 'The PHI2 Method: A way to assess time-variant reliability using time-invariant reliability tools'. *Proc. European Safety and Reliability Conference ESREL'02*: pp. 472-479. Lyon.
- [9] Allix, O., Corigliano, A. "Geometrical and interfacial non-linearities in the analysis of delamination in composites". *Int. J. of Solids and Structures*, 36, 2189-2216, 1999.
- [10] Alfano, G., Crisfield, M.A. "Finite element interface models for the delamination analysis of laminated composites". *Mechanical computational issues. International journal for numerical methods in engineering*, 50pp 1701-1736, 2001.
- [11] Valoroso, N., Champaney, L. "Evaluation of interface models for the analysis of non-linear behaviour of adhesively bonded joints". *European Conference Computational Mechanics*. Poland, 2001.
- [12] Ripling, E.J., Mostovoy, S., Patrick, R.L., "Measuring fracture toughness", *J. Mater* (pp 239-265, 1967.
- [13] Kinloch, A.J., Blackman, B.R.K., "Fracture tests for structural adhesive joint, in fracture mechanics testing methods for polymers, adhesives and composites", Eds. A.Pavan, D.R.Moore and J.G.Williams, Elsevier science, Amsterdam, 2001.
- [14] Davies, P., Sargent, J.P., "Fracture Mechanics tests to characterize bonded glass/epoxy composites: application to strength prediction in structural assemblies", 3rd ESIS, Elsevier, 2003
- [15] Kinloch, A.J., Blackman, B.R.K., Parashi, M., Teo, W.S., "Measuring the mode I adhesive fracture energy GIC, of structural adhesive joints: the results of an international round-robin".